Synthesis and unambiguous NMR characterization of linear and branched *N*-alkyl chitosan derivatives.

Casper Van Poucke*, Evert Verdegem, Sven Mangelinckx, Christian V. Stevens

Department of Green Chemistry and Technology, Faculty of Bioscience Engineering, Ghent University, Coupure Links 653, B-9000 Ghent, Belgium.
E-mail address: casper.vanpoucke@ugent.be (C. Van Poucke)
Telephone number: +32 9 264 5860 (Belgium)

Abstract

Chitosan, sourced from abundant chitin-rich waste streams, emerges as a promising candidate in the realm of future functional materials and chemicals. While showing numerous advantageous properties, chitosan sometimes falls short of competing with today's non-renewable alternatives. Chemical derivatization, particularly through *N*-alkylation, proves promising in enhancing hydrophobic functionalities. This study synthesizes fifteen chitosan derivatives (degree of substitution = 2-10 %) using an improved reductive amination method. Next, selective depolymerization through acid hydrolysis reduced the chain rigidity imposed by the polymer backbone. This facilitated unambiguous structural characterization of the synthesized compounds using a combination of common NMR techniques. Two potential side reactions are identified for the first time, emphasizing the need for detailed structural information to unlock the true potential of these derivatives in future applications.

Hypothesis

The increase in chain mobility induced by the selective depolymerization of aliphatic *N*-alkyl chitosan derivatives allows for an unambiguous NMR characterization.

1. Introduction

Chitin is a class of widely available, linear, non-toxic and biodegradable polysaccharides. Chitin is naturally present in the exoskeleton of crustaceans, the fungal cell wall and the structural components of insects, making it the second most abundant natural biopolymer. Chitin can easily be extracted from secondary leftover waste streams, due to its wide availability, making it ever more attractive (Triunfo et al., 2022). Chitin mainly consists of β(1→4) linked *N*-acetyl-D-glucosamine units, with a few percentages of β(1→4) linked D-glucosamine building blocks. Chitin is generally transformed into chitosan through deacetylation to improve its versatility and aqueous solubility. Chitosan is also non-toxic, biodegradable and biocompatible, while free amino groups afford natural antimicrobial and antifungal activities. However, this activity is limited in water at physiological pH as the available amino groups need to be sufficiently protonated for chitosan to dissolve ($pK_a \approx 6$-8) (Anthonsen & Smidsrød, 1995).

The selective addition of aliphatic side chains onto the amino groups of chitosan produces an interesting class of chitosan derivatives called *N*-alkyl chitosans, named after their *N*-alkyl amine counterparts. These amphiphilic compounds, which are mostly obtained through reductive amination, have been applied in numerous fields as viscosity modifiers (Desbrières et al., 1996), hemostatic agents (Dowling et al., 2011), wood additives(Mati-Baouche et al., 2019), emulsifiers (Kalliola et al., 2018), edible food coatings (de Britto & de Assis, 2007), drug delivery agents (Benediktsdóttir et al., 2014) and recently even as algal flocculants (Demir-Yilmaz et al., 2023).

Another interesting application that makes use of their amphiphilic nature is as antimicrobial agents. As chitosan mostly interacts with the microbial outer surface, it is hypothesized that the addition of hydrophobic aliphatic side chains might aid in these types of interactions as well as broaden the

applicable pH range (Kong et al., 2010). However, most structure-activity studies focus on excessively alkylated derivatives or present scattered single data points that are difficult to compare with one another (Paula et al., 2020)(Ma et al., 2008). For these excessively alkylated derivatives, quaternization is required to enable aqueous bio-testing, making it hard to decouple the effects of both structural modifications afterward (Sahariah et al., 2015)(Kim et al., 1997)(Jia et al., 2001). Hence, structure-activity studies of the biological effects on microorganisms of different types of *N*-alkyl modifications without subsequent quaternization, are scarce. This makes the exact effect on the antimicrobial activity of adding hydrophobic chains rather elusive (Sahariah & Másson, 2017).

In the current study, the almost 30-year-old reductive amination protocol was revisited and given a modern update towards a more scalable and less environmentally taxing process. The subsequent protocol was applied to synthesize a library of fifteen different linear and branched *N*-alkyl chitosans, of which several new derivatives, with an envisioned degree of substitution (DS) of 10 %. This low substitution ensured a similar solubility profile as native chitosan without the need for subsequent quaternization. Subsequently, these derivatives were selectively depolymerized to enable an unambiguous elucidation of the structure of thirteen compounds and indications for the other two. Moreover, this further led to the identification of two side reactions for the first time. These include the *N*-isopropylation of the chitosan backbone during product isolation, as well as the acid-catalyzed hydration of unsaturated side chains on the chitosan backbone. Guidelines for the NMR characterization of this class of compounds are presented, aiming to serve as a welcome reference for future studies, enabling an unambiguous correlation between structure and activity in the future.

2. *Results and discussion*

2.1. *N*-alkyl chitosans and their NMR characterization: state of the art

The degree of substitution (DS) is one of the most important structural parameters for chemically modified chitosan. Most of the time, the DS is derived from relative ^{1}H NMR integration, which makes it heavily reliant on the correct peak assignment thereof. However, a fact that is quite often overlooked within the literature regarding *N*-alkyl chitosans is the employed conditions during NMR analysis, especially ^{1}H NMR analysis. To dissolve chitosan or its hydrophobic *N*-alkylated counterparts in (deuterated) water, acidic conditions are required. Subsequently, most of the amino groups on the chitosan chain will be protonated during aqueous NMR analysis. However, this significantly influences the chemical ^{1}H NMR shift of the neighboring 1' methylene/methine protons next to these protonated amino groups. This phenomenon is well established for structurally similar *N*-alkyl amines, as downfield shifts of about 0.5-1 ppm can be observed in ^{1}H NMR due to the decreased shielding of the α methylene/methine proton(s) next to the protonated positively charged ammonium ion relative to those of the uncharged amine (Ma & Warnhoff, 1965). This effect is relatively less pronounced in ^{13}C NMR (Sarneski et al., 1975). This has led to seemingly two different types of ^{1}H NMR peak assignments for these *N*-alkyl chitosans (Figure 1). On one hand, all of the aliphatic proton signals are assigned to the different signals observed within the 0-2 ppm region, including the 1' protons next to the protonated amino groups (Bobu et al., 2011)(Rabea et al., 2005)(Sajomsang et al., 2009)(Venkataraman et al., 2013). On the other hand, the 1' protons are assigned about 1-2 ppm downfield, overlapping with the two distinct H_2 signals of the derivative (Desbrières et al., 1996)(Kurita & Isogai, 2010)(Sashiwa & Shigemasa, 1999). Following the reasoning above, we hypothesize the latter to be correct. Furthermore, looking at the example depicted in Figure 1, simple integration of the signals between 0-2 ppm in ^{1}H NMR gives an integral ratio of about 3:2:1.6, which is very close to the theoretical value of 3:2:2 if the 1' protons are assigned downfield. A more in-depth discussion regarding this matter will follow later (see Section 2.3.).

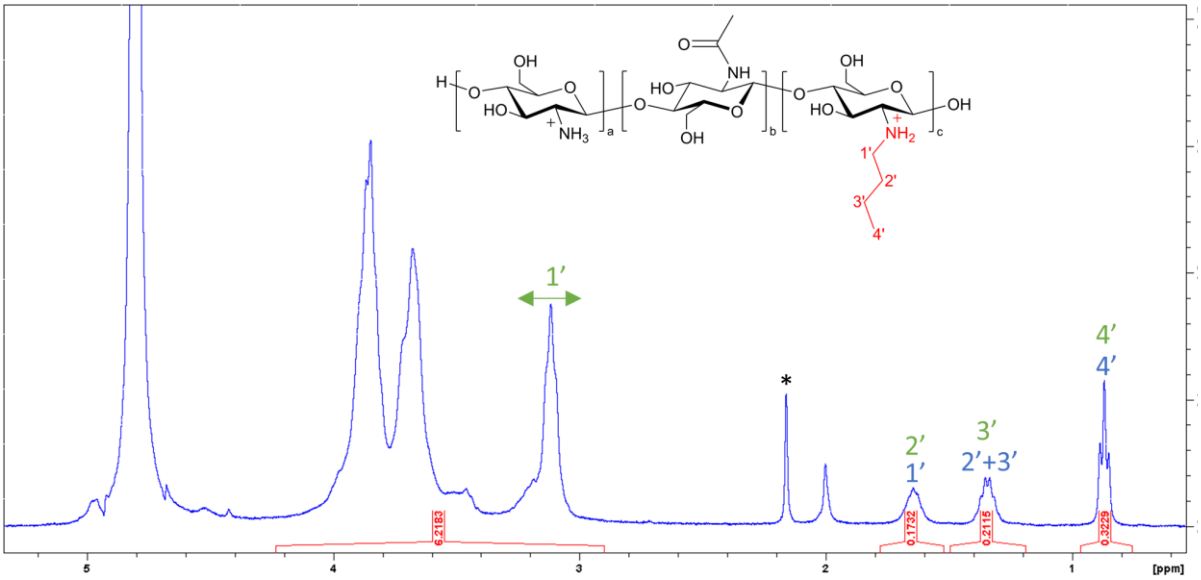

*Figure 1. ^{1}H NMR (400 MHz) spectrum of N-butyl chitosan (DS_{ch} = 10 %, based upon ^{1}H NMR integration, see Section S4.) at 20 mg/mL in 1 vol% d-TFA in D_2O, together with the two most popular structural assignments present in literature, indicated in green and blue. Acetone as a minor impurity is indicated with an *.*

2.2. Synthesis of *N*-alkyl amines via reductive amination

Within this study, we aim to synthesize fifteen different hydrophobic *N*-alkyl chitosans with an envisioned DS of 10 %. All of these derivatives need to be soluble in aqueous media to facilitate NMR analysis in acidic D_2O, as well as aqueous biotesting in the future. This DS was chosen because, early on, we observed, as did several other groups (Lepeltier et al., 2015)(Desbrières et al., 1996)(Sajomsang et al., 2008)(Demir-Yilmaz et al., 2023), that derivatives with too high of a DS become insoluble in acidic aqueous media. This phenomenon is especially prevalent when the added chains become more hydrophobic. Moreover, similar DS values are desirable as they will enable the study of the effects of the different groups added, establishing preliminary structure-activity relationships (SAR) in the future.

The reductive amination developed by Hall and Yalpani (Yalpani & Hall, 1984) and refined by Rinaudo, Desbières and Martinez (Desbrières et al., 1996) is by far the most utilized method to synthesize these hydrophobic *N*-alkyl chitosan derivatives. However, yet effective, this method has two major drawbacks: toxic $NaCNBH_3$ is utilized as the reducing agent and an almost 50/50 mixture of organic solvent (EtOH, MeOH or DMF) and water is required for the reaction to proceed effectively (Sashiwa & Shigemasa, 1999) (Sajomsang et al., 2008).

To try and alleviate some of the environmental burden accompanied by the production of these compounds and to move towards a more scalable process while still obtaining qualitative products in the end, several different reaction conditions and isolation methods were explored (see Sections S1. and S2.). Afterward, the recently proposed (Cok et al., 2020)(Cosenza et al., 2011) α-picoline borane complex (PICB) was selected based on the GSK reagent selection guide for reductive aminations as the preferred reducing agent over the problematic $NaCNBH_3$ (Adams et al., 2013). Acidic water containing low amounts of cetylpyridinium chloride (CPC) was selected as an alternative solvent to the mixed solvent systems, as water is still the preferred solvent of choice in many cases (Prat et al., 2016). Any residual PICB was quenched by acidifying and heating the sample and a pure product was obtained by precipitation with an excess of acetone. Furthermore, utilizing this methodology, no significant molecular weight reduction could be observed for the derivatives compared to the chitosan starting material (see Section S3.).

Next, a relationship between the obtained DS and the added equivalents of aldehyde (see Figure 2) was established for these newly applied conditions. As expected, as the DS increased, the aqueous solubility worsened, especially for samples with a DS > 25 %.

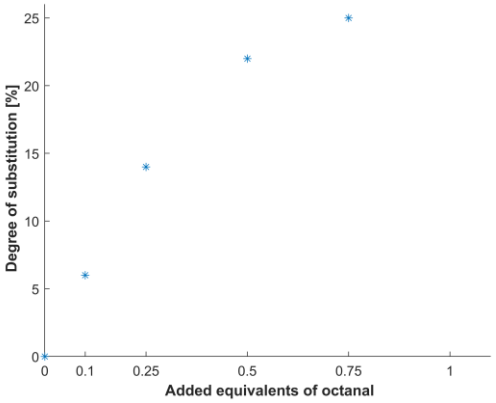

Figure 2. The relationship between the observed DS (based upon ^{1}H NMR integration, see Section S4.) and the added equivalents of aldehyde. Octanal was selected as a representative long, linear and aliphatic aldehyde that is practically insoluble in water. No DS was calculated for the product obtained after the addition of 1 equivalent octanal as the product became insoluble in aqueous media. In every experiment, the same amount of equivalents of PICB were added as the equivalents of aldehyde.

Finally, a particularly interesting ^{1}H-^{1}H COSY coupling was observed when, by accident, the quenching step was omitted. This coupling indicated the presence of *N*-isopropyl groups onto the chitosan chain (Kurita & Isogai, 2010), next to the envisioned *N*-alkyl substituent (see Figure 3). This product originates from the covalent grafting of acetone onto chitosan, which is used for the precipitation of the chitosan derivative (see Section 4.4.). This process occurs via a reductive amination facilitated by leftover PICB. Therefore, to avoid unwanted side reactions during product isolation, we would like to stress the importance of quenching the residual PICB after the reaction has finished.

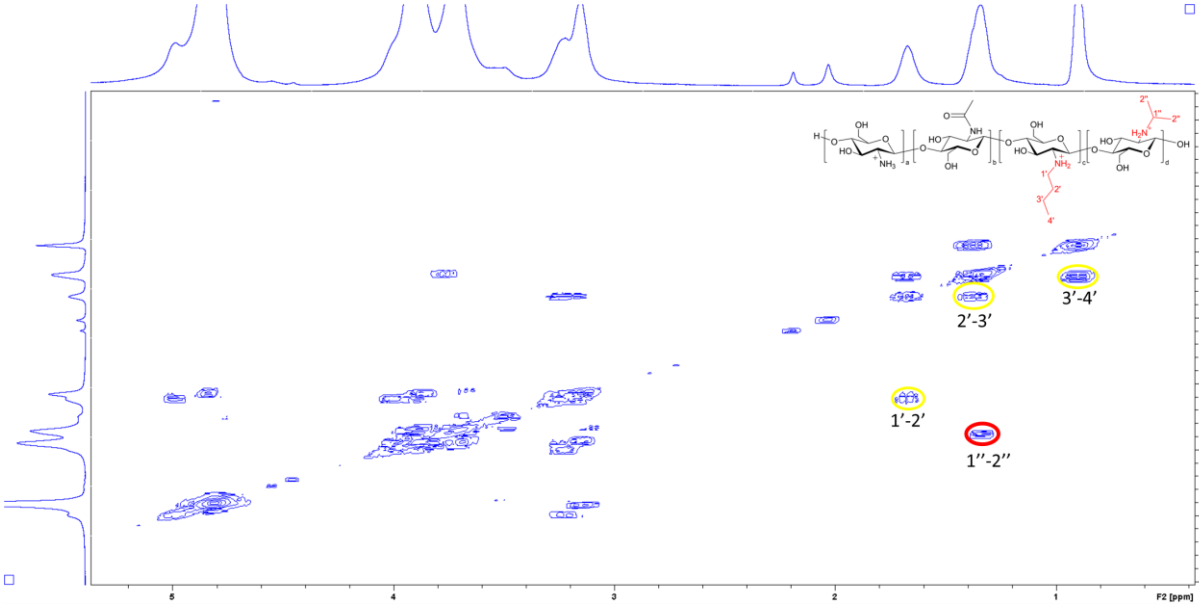

Figure 3. ^{1}H-^{1}H COSY NMR (400 MHz) spectrum of N-butyl chitosan contaminated with N-isopropyl groups ($DS_{ch,\ butyl}$ = 24 %, $DS_{ch,\ isopropyl}$ = 9 %, based upon ^{1}H NMR integration, see Section S4.) at 20 mg/mL in 1 vol% d-TFA in D_2O. The ^{1}H-^{1}H couplings of the different side chains are indicated in yellow for N-butyl and red for N-isopropyl groups.

2.3. Structural elucidation of the obtained derivatives

To enable a full and unambiguous structural characterization, *N*-butyl chitosan (DS = 10 %, based upon ^{1}H NMR integration, see Section S4.) was synthesized as a model compound. 1 vol% d-TFA in D_2O was selected as the NMR solvent of choice as this generally gave the best resolution for all the obtained 1D and 2D NMR data.

2.3.1. Direct one and two-dimensional NMR analysis

Unfortunately, the ^{1}H-^{1}H COSY spectrum of the *N*-butyl chitosan sample at 20 mg/mL showed no conclusive evidence of the position of the 1' protons in ^{1}H NMR either. All expected ^{1}H-^{1}H couplings between neighboring protons on the added backbone were present, except the coupling between the 1' protons and their neighboring 2' protons. Most likely, the limited mobility of these 1' protons, as these are the closest to the chitosan backbone, together with the low degree of substitution caused this signal to dissipate in the noise. Hence, an obvious first solution would be to increase the degree of substitution by increasing the equivalents of aldehyde added (see Figure 2), as can be seen in Figure 3. However, for longer *N*-alkyl chitosan the degree of substitution has an upper solubility limit (*vide infra*), making this a not viable solution for all fifteen derivatives. Therefore, it was hypothesized that a significant reduction in polymer molecular weight would improve the overall mobility of the entire molecule, including the 1' atoms of the added side chain, relatively increasing the signal strength of all atoms with previously limited mobility compared to the more mobile 3' and 4' outer proton signals.

2.3.2. Molecular weight reduction of N-alkyl chitosan towards N-alkyl COS

Two well-described chemical methods for the production of chitooligosaccharides (COS) were evaluated for the direct and selective cleavage of modified *N*-alkyl chitosans towards *N*-alkyl COS. These methods are oxidative cleavage with $NaNO_2$ (Allan & Peyron, 1995)(Tømmeraas et al., 2001) and acidic hydrolysis with concentrated HCl (Vårum et al., 2001). To our knowledge, this approach to obtain *N*-alkyl COS was not described before, as generally COS are produced first and modified afterward.

2.3.2.1. Oxidative $NaNO_2$-mediated depolymerization

The oxidative HONO cleavage showed very reproducible results for non-modified chitosan, as numerously described before (Chapelle et al., 2019)(Coudurier et al., 2020)(Mo et al., 2020). However, despite these promising early results, an *N*-butyl chitosan sample yielded a very heterogeneous product, which only partly dissolved after depolymerization. Moreover, several new peaks appeared in the 0-2 ppm region within the ^{1}H NMR spectrum (see Section S5.), further indicating a complex product mixture. As previously described by Allan and Peyron (Allan & Peyron, 1995), cleavage only occurs at the primary amino groups of chitosan, which are subsequently deaminated, generating a 2,5-anhydro-D-mannose unit on one side and cleaving the glycosidic bond in the process (see Figure 4). However, as secondary *N*-alkyl amino units are present, nitrosamines could be generated, which might be one of the factors contributing to the observed complex behavior. Next to this, if the cleavage selectively occurs only on the primary amino groups of chitosan, degrading them in the process, there will be a relative increase in *N*-alkyl chains in certain COS fractions, severely limiting their further acidic aqueous solubility. This could further explain the heterogeneous nature of the depolymerization products. No further attempts were made utilizing this method, as the heterogeneous nature of the obtained products, instead of simplifying analysis, further complicated subsequent NMR analysis.

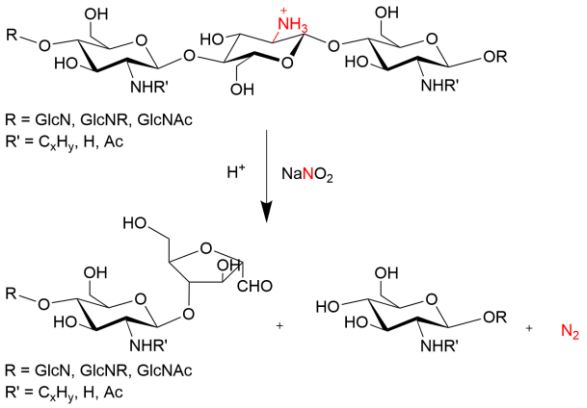

Figure 4: The oxidative $NaNO_2$-mediated cleavage of chitosan.

2.3.2.2. Acid hydrolysis of chitosan in concentrated DCl/HCl

Initially, depolymerization experiments were conducted directly in 2M DCl for 24 hours under reflux conditions. This had three major advantages:

- The samples could be analyzed directly afterward by NMR.
- The resonance of the residual solvent peak (HOD) does not interfere with any of the anomeric carbohydrate signals as the high acidity of the sample induced a strong downfield shift (Einbu & Vårum, 2007)(P. Wang et al., 2021).
- At this DCl concentration, the rate of deacetylation is similar to the rate of depolymerization (Einbu & Vårum, 2007). This resulted in fully deacetylated samples, yielding a more uniform copolymer with only two different monomers instead of three, further simplifying subsequent (especially ^{13}C) NMR analysis.

However, no pure COS could be obtained this way as indicated by NMR (see Sections S6. and S9.). Several new impurities could be observed in both ^{1}H NMR and especially in ^{13}C NMR when comparing these spectra with existing literature (Domard & Cartier, 1989)(Fukamizo et al., 1991)(Sugiyama et al., 2001). We hypothesize that most of these impurities are remnants of the remaining chitin-glucan complex within the utilized chitosan of fungal origin (*Aspergillus niger* biomass). This aqueous insoluble complex is naturally present in fungal biomass and is prone to acidic degradation (Farinha et al., 2015). The presence of several different types of glucans or even glucose could explain most of these signals which are situated in the 50-100 ppm region in ^{13}C NMR.

Additionally, the automatic tuning and matching (ATMA) of our NMR probe was no longer an option as a result of the high ionic strength of the solvent (Einbu & Vårum, 2008), worsening all subsequent NMR analysis and even rendering proper two-dimensional ^{1}H-^{13}C HSQC analysis impossible. As these analyses are a vital part of the structural elucidation of our obtained compounds, we decided to use 1 vol% d-TFA in D_2O as our NMR solvent system instead.

Selective precipitation of the longer COS fraction was performed by the addition of five volumes of acetone to the hydrolysate (obtained in 2M HCl after 24 hours under reflux conditions), to further simplify subsequent NMR analysis. A second fraction precipitated upon the addition of excess acetone. Further ^{1}H NMR and especially ^{13}C NMR analysis confirmed the purity of the obtained longer COS fraction without any of the previously observed impurities (see Sections S7. and S10.). For our second isolated fraction, a mixture containing a large amount of short water soluble β(1,3)-glucans is suggested based upon the comparison of our obtained ^{1}H NMR data with the ^{1}H NMR data of the isolated fraction obtained in the work of Hanashima et al. (see Section S8.) (Hanashima et al., 2014).

2.3.3.Structural NMR analysis of N-alkyl COS

Based on the considerations above, the following workflow was used to obtain fifteen *N*-alkyl COS, which were subsequently subjected to one-dimensional ^{1}H, ^{13}C and DEPT-135 NMR and two-dimensional ^{1}H-^{1}H COSY and ^{1}H-^{13}C HSQC NMR analysis.

- Synthesis of the aliphatic *N*-alkyl chitosan via reductive amination.
- *N*-isopropylation check via ^{1}H-^{1}H COSY NMR analysis.
- Depolymerization of the aliphatic *N*-alkyl chitosan towards its respective *N*-alkyl COS.
- Precipitation of the longer COS.HCl fraction with five reaction volumes of acetone.
- NMR analysis of the dried precipitate.

Due to the short chain length of the obtained COS compared to the original chitosan, the internal units could be differentiated from their corresponding reducing (α and β) and non-reducing ends (see Figure 5).

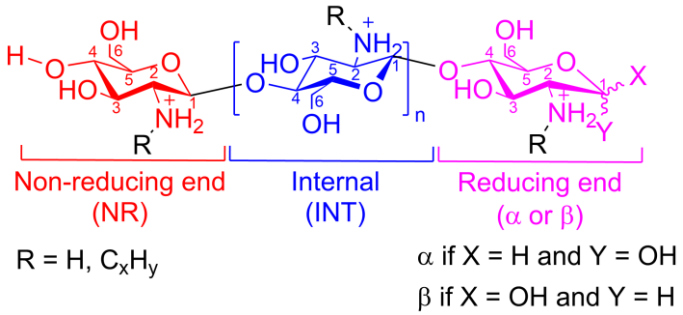

Figure 5. Schematic overview of the produced N-alkyl COS. The introduced color scheme will be adapted in all subsequent NMR analyses.

2.3.3.1. The example of *N*-2-ethylbutyl COS

N-2-ethylbutyl chitosan (DS = 10 %, based upon ^{1}H NMR integration, see Section S11.10.) was selected as a representative example. All NMR analyses of the remaining fourteen derivatives are supplied in the supplementary information (see Section S11.). Similar patterns, as described below, were observed for all samples, except for unsaturated *N*-alkyl chitosan derivatives (*vide infra*). Additionally, tables containing all the observed chemical shifts (^{1}H and ^{13}C NMR) are supplied within the supplementary information (see Section S13.).

First, all ^{13}C signals of non-modified units were assigned based on previously published literature (Domard & Cartier, 1989)(Fukamizo et al., 1991). Next, all new signals of modified units were assigned based on their hypothesized structure (see Figure 6). Additionally, DEPT135 (Distortionless Enhancement by Polarization Transfer) was utilized to further verify the nature (CH/CH_3 or CH_2) of all newly assigned ^{13}C signals (see Section S11.10.). For the aliphatic 2-ethylbutyl side chain, the obtained ^{13}C shifts of 49.3, 37.6, 22.7/22.4 and 9.8/9.3 ppm are in good agreement with previously reported data (de Britto & de Assis, 2007)(Sashiwa & Shigemasa, 1999), as well as reported values for protonated aqueous alkylamines (Sarneski et al., 1975). However, the chemical shifts of the carbon atoms on the 1-6 positions of the modified internal COS units, rather than the chemical shifts of the 1'-4' positions of the attached alkyl chain, are much harder to assign, and we did not manage to find any direct data to compare our results with. Yet, despite being overlooked quite often, in theory, the resonance signals of neighboring carbon atoms are expected to shift if the amino group on the 2 position is modified because of the covalent attachment of the added side chain. A chemical shift of 96.1, 68.7, 61.6 and 60.7 ppm was observed for the carbon atoms at the 1, 3, 2 and 6 positions of the modified internal COS units. When comparing these results with our previously obtained data for lowly modified (DS = 20 %)

N-sulfopropyl chitosan (Van Poucke et al., 2023), very similar values of 96.5 and 61.5 ppm were obtained for the carbons situated on the 1 and 2 positions, respectively, of the modified chitosan units.

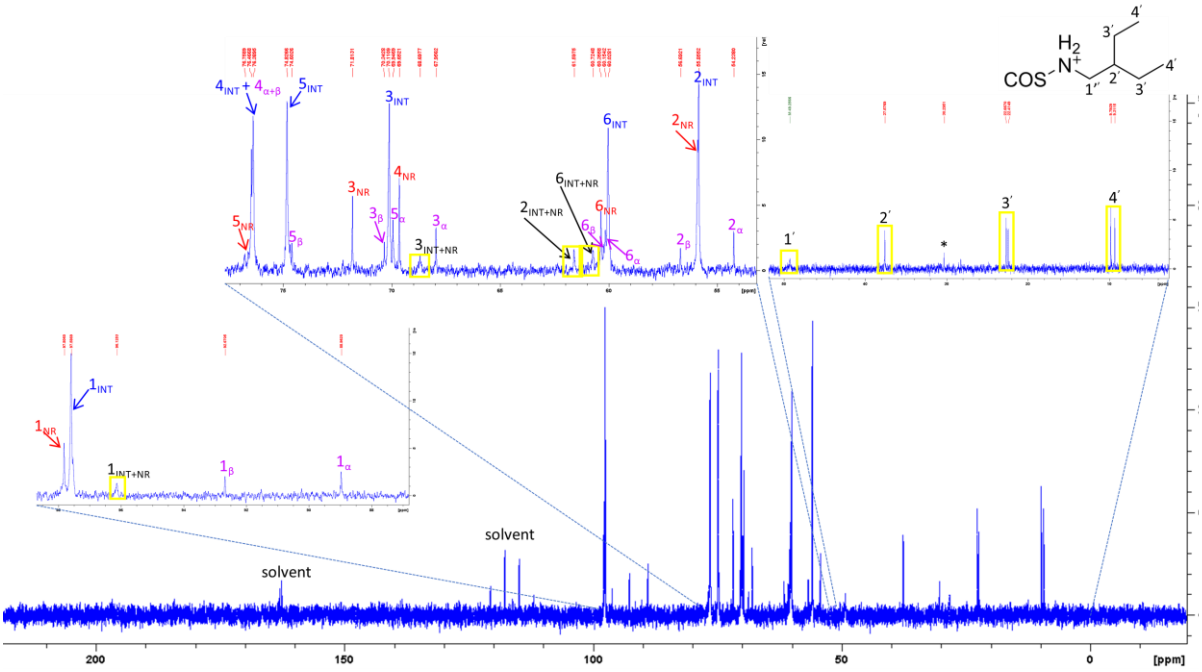

*Figure 6. ^{13}C NMR (100.6 MHz) spectrum of N-2-ethylbutyl COS (DS_{COS} = 9 %, based upon ^{1}H NMR integration, see Section S11.10.) at 20 mg/mL in 1 vol% d-TFA in D_2O. The color scheme introduced in Figure 5 was adapted for all non-modified units. Signals of modified units are indicated in yellow. Acetone as a minor impurity is indicated with an *.*

Based upon the ^{13}C chemical shifts, proton signals in ^{1}H NMR were assigned via their respective ^{1}H-^{13}C HSQC (Heteronuclear Single Quantum Coherence) NMR correlation (see Figure 7). Next, the ^{1}H NMR chemical shifts of the non-modified internal and external units were cross-checked with existing literature (Sugiyama et al., 2001). For the added aliphatic side chain, the obtained chemical shifts of 3.14, 1.67, 1.39 and 0.85 ppm are in good agreement with previously reported data for aliphatic *N*-alkyl chitosan derivatives (Desbrières et al., 1996) as well as protonated aqueous alkylamines (Ma & Warnhoff, 1965). Notably, the data unambiguously shows the exact ^{1}H NMR chemical shift of 3.14 ppm for the 1' protons, which undergo a significant downfield shift due to the protonation of the secondary amino group. Furthermore, a similar argument can be made for ^{1}H NMR as for ^{13}C NMR for the 1-6 positions of the modified internal COS units. The proton on the 1_α anomeric position of the modified external COS units exhibits a chemical shift of 5.54 ppm, while the protons on the 1, 3, and 2 positions of the modified internal COS units show chemical shifts of 5.02, 4.05, and 3.24 ppm, respectively. Additionally, the ^{1}H NMR chemical shift of the proton on the 2 position of the modified internal COS unit closely aligns with our previous work (Van Poucke et al., 2023) and with findings from Kurita and Isogai (Kurita & Isogai, 2010).

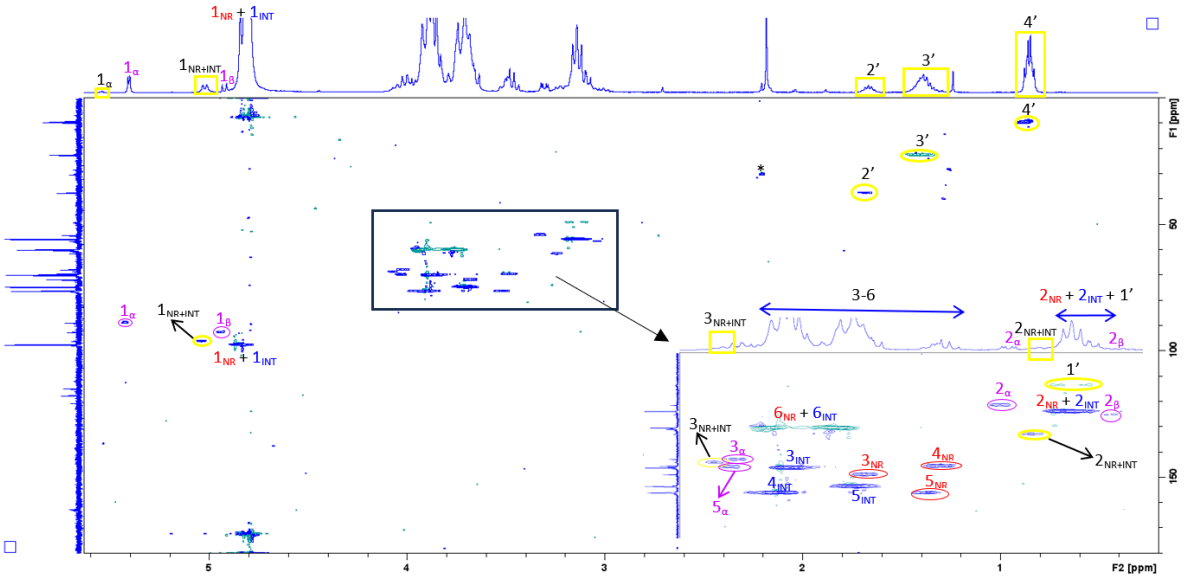

*Figure 7. ^{1}H-^{13}C HSQC NMR (400 MHz) spectrum of N-2-ethylbutyl COS (DS_{COS} = 9 %, based upon ^{1}H NMR integration, see Section S11.10.) at 20 mg/mL in 1 vol% d-TFA in D_2O. The color scheme introduced in Figure 5 was adapted for all non-modified units. Signals of modified units are indicated in yellow. CH_2 signals are indicated in green and CH/CH_3 signals in blue. Acetone as a minor impurity is indicated with an *.*

Next, these ^{1}H NMR assignments were verified via ^{1}H-^{1}H COSY (COrrelation SpectroscopY). The most important ^{1}H-^{1}H couplings are assigned in Figure 8. This leads to the following conclusions:

- The presence of new 1-2 and 2-3 couplings of the protons on the internal and external reducing units, indicates that a certain percentage of the amino groups of COS are indeed covalently modified.
- The proton coupling along the added side chain (1' to 4') indicates the covalent attachment of an *N*-2-ethylbutyl group.

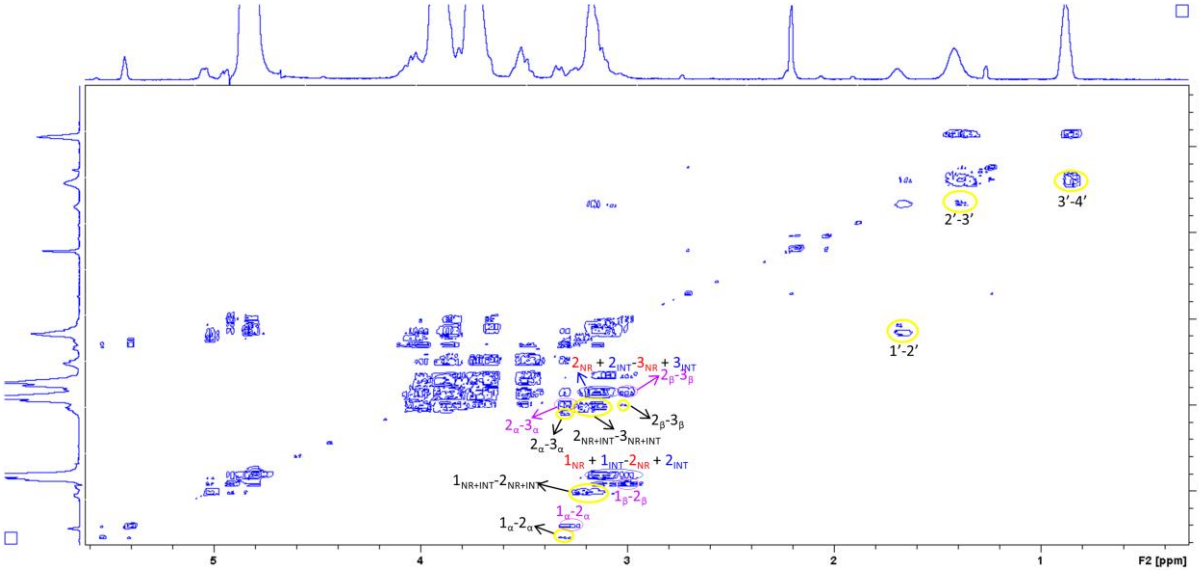

Figure 8. ^{1}H-^{1}H COSY NMR (400 MHz) spectrum of N-2-ethylbutyl COS (DS_{COS} = 9 %, based upon ^{1}H NMR integration, see Section S11.10.) at 20 mg/mL in 1 vol% d-TFA in D_2O. The color scheme introduced in Figure 5 was adapted for all non-modified units. Signals of modified units are indicated in yellow.

Unfortunately, no direct coupling between the 1' position of the added side chain and the 2 position on the chitosan backbone could be observed via additional ^{1}H-^{13}C HMBC (Heteronuclear Multiple Bond Correlation) analysis (see Section S12.). Nevertheless, based on the arguments above, the direct covalent attachment of the *N*-2-ethylbutyl group is evident.

Finally, the carbons and protons at positions 3' and 4' show an interesting behavior. When solely looking at the structure of the attached *N*-2-ethylbutyl group while neglecting the chiral COS backbone, one could assume that the carbons and protons on either side of the chain are chemically equivalent. However, this seems not to be the case as evidenced by the two signals at 9.3 and 9.8 ppm for the carbons at the 4' position and 22.4 and 22.7 ppm for the carbons at the 3' position in Figure 6. Additionally, the signal in Figure 7 at 0.85 ppm for the protons at the 4' position shows a more complex multiplicity instead of the expected triplet. The observed differences are most likely due to several different processes, some of which are temperature dependent as well as the inherent diastereotopic relationship of the substituents due to the presence of the chiral COS backbone. To further study this behavior, the signal at 0.85 ppm in ^{1}H NMR at 298 K was compared with the corresponding signal at 308, 328 and 343 K. In Figure 9, a temperature-dependent behavior can be observed, in which signal broadening is reduced as the temperature increases. This is most likely due to the reduced influences of several temperature-limited processes. An example might be the limited mobility of the chiral COS backbone, which could impose steric constraints on the added side chain, which is reduced at higher temperatures. However, in theory, at any given temperature, some small difference should remain, as observed for several chiral alkyl amines in the past, due to the previously mentioned diastereotopic relationship (Ando et al., 1979).

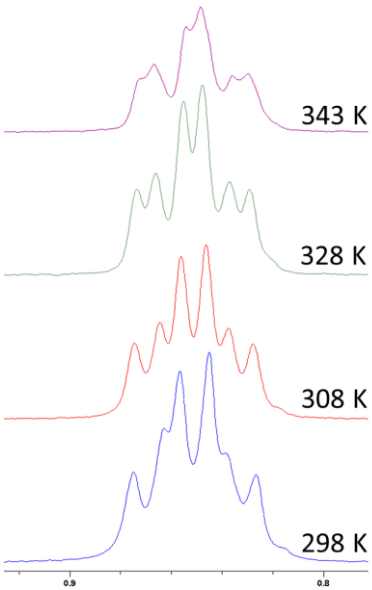

Figure 9. Zoom of the 0.8-0.9 ppm region of the ^{1}H NMR (400 MHz) spectrum of N-2-ethylbutyl COS (DS_{COS} = 9 %, based upon ^{1}H NMR integration, see Section S11.10.) at 20 mg/mL in 1 vol% d-TFA in D_2O at 298, 308, 328 and 343 K.

2.3.3.2. The particular case of unsaturated *N*-alkyl chitosan derivatives

Figure 10 depicts the ^{1}H-^{13}C HSQC NMR spectrum obtained after acid-mediated depolymerization of *N*-pent-4-enyl chitosan (DS_{ch} = 7 %, based upon ^{1}H NMR integration, see Section S11.7.). Within the spectrum (based on their expected chemical shifts and the HSQC phasing) there is a terminal methyl group at the 5' position present instead of the expected terminal methylene group, indicating a modification on the added side chain during the depolymerization reaction. Based upon the data presented in Figure 10, we hypothesized that the alkene moiety was hydrated under the thermal aqueous acidic conditions. This was further confirmed by additional ^{1}H, ^{13}C, ^{1}H-^{1}H COSY, ^{1}H-^{13}C HMBC

and DEPT135 NMR analyses, both before and after depolymerization, confirming the structure of the original *N*-pent-4-enyl chitosan and the subsequently formed *N*-4-hydroxypentyl COS (see Sections S11.7. and S11.8.).

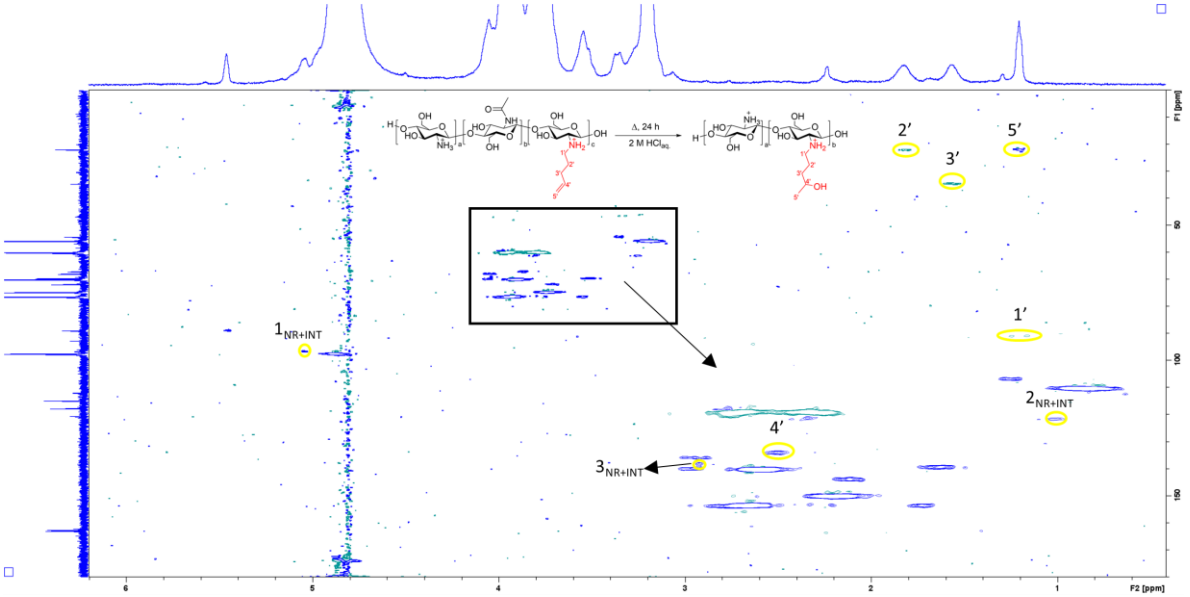

Figure 10. ^{1}H-^{13}C HSQC NMR (400 MHz) spectrum of N-4-hydroxypentyl COS (DS_{COS} = 4 %, based upon ^{1}H NMR integration, see Section S11.8.) at 20 mg/mL in 1 vol% d-TFA in D_2O. Signals of modified units are indicated in yellow. CH_2 signals are depicted in green and CH/CH_3 signals in blue.

The addition of the hydroxyl group at the 4' position because of the higher stability of the intermediate secondary carbocation is a textbook example of Markovnikov's rule. Logically, substituted alkenes should react faster because of the formed intermediate tertiary carbocation. Hence, the reductive amination of chitosan with natural monoterpenoid aldehydes containing prenyl groups should yield substrates that are easily hydrated. To this extent, two natural aldehydes, citral and citronellal, were reductively aminated to chitosan. However, the exact structure of the obtained compounds after depolymerization could not be determined via NMR analysis because neither of the added sidechains gave sufficiently strong signals during analysis. Only the expected covalent addition could be confirmed (see Sections S11.15. and S11.16.). Yet, solely based on ^{1}H NMR analysis of the chitosan-citronellal adduct (see Figure 11), the following structures are proposed. Before depolymerization, only a fraction of the prenyl groups of the added side chain remains intact while the rest is hydrated. This is evidenced by the presence of four different methyl groups while the original aldehyde has three. To explain this odd observation, we propose the methyl assignment, based on their expected chemical shifts, depicted in Figure 11. The two methyl groups on the original prenyl group are observed at the most downfield positions, specifically at 1.67 and 1.60 ppm, while the remaining methyl group is situated at the most shielded position, resonating at 0.89 ppm. The methyl groups on the hydrated prenyl group overlap and resonate at an intermediate value of 1.17 ppm. Additionally, there is a small signal of the methyne proton of the prenyl group present at 5.18 ppm. Unsurprisingly, after depolymerization, the obtained product is fully saturated (see Figure 11 and Section S11.15.). Based upon the disappearance of the two methyne protons at 5.27 and 5.16 ppm after the depolymerization of the chitosan-citral adduct (See Figure 11), a similar behavior is expected. We hypothesize that the initial hydration took place during the quenching of residual PICB (see Section 4.4.) as the mixture was acidified and heated. A similar selective acid-catalyzed hydration was observed by Ishino and Kumanotani for several citronellal-amine adducts towards hydroxycitronellal (Ishino & Kumanotani, 1974). The observations above could also be of particular interest when essential oils are utilized as green aldehyde feedstocks as in the work of Paula et al. (Paula et al., 2020), as FTIR analysis, qualitative Baeyer-tests and ^{1}H NMR

analysis indicated the presence of unsaturation in the obtained chitosan derivatives. However, during their ^{1}H-^{13}C HSQC NMR analysis not even a trace of unsaturation was observed. The fact that their ^{1}H-^{13}C HSQC NMR analysis was performed at 70 °C under acidic conditions, in contrast with the shorter ^{1}H NMR analysis which was performed at room temperature, might be a possible explanation for this rather strange observation, as most prenyl groups could have been hydrated during the HSQC analysis.

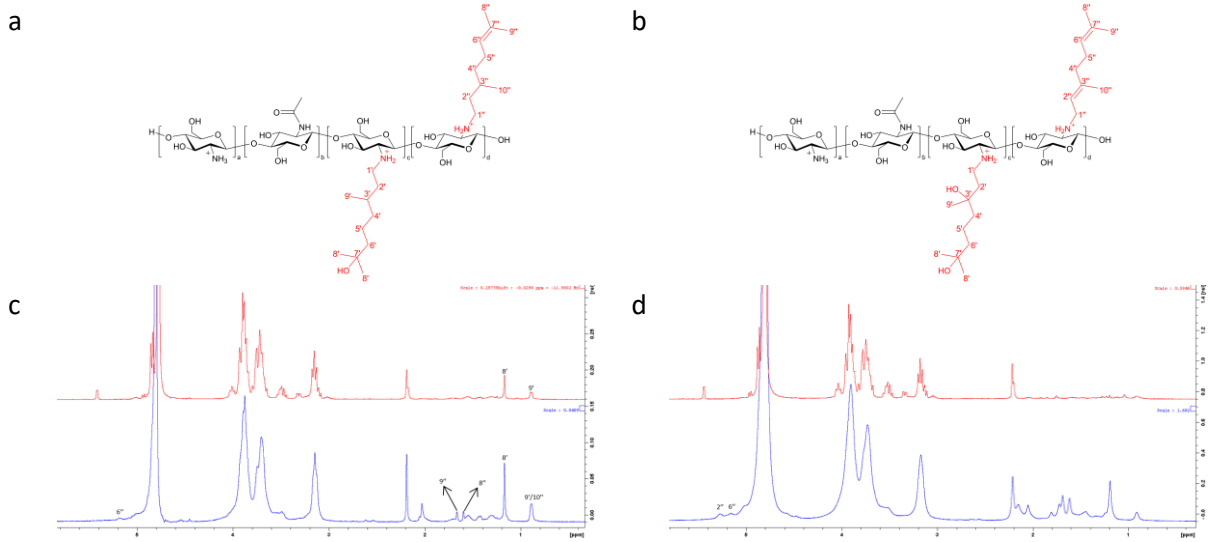

Figure 11. The proposed chemical structures for the chitosan-citronellal adduct (a) and the chitosan-citral adduct (b) before depolymerization are depicted. ^{1}H NMR (400 MHz) spectrum of the chitosan-citronellal adduct (c) (DS_{ch} = 5 % and DS_{COS} = 3 %, based upon ^{1}H NMR integration, see Section S11.15.) and chitosan-citral adduct (d) at 20 mg/mL in 1 vol% d-TFA in D_2O, before (blue) and after (red) depolymerization.

2.4. Overview of the synthesized N-alkyl chitosans and their COS derivatives.

*Table 1. An overview of the synthesized N-alkyl chitosans, their COS derivatives, and their calculated DS values based upon ^{1}H NMR integration. The displayed standard deviations are based on the interpeak ^{1}H NMR variance. The samples of which the added side chain structurally changed during depolymerization are indicated with an * (see section 2.3.3.2.). N.D. = not-determined; DS_{ch} = degree of substitution of the chitosan sample; DS_{COS} = degree of substitution of the COS sample.*

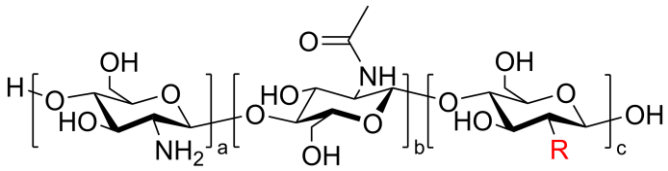

R =	DS_{ch} (%)	DS_{COS} (%)	R =	DS_{ch} (%)	DS_{COS} (%)	R =	DS_{ch} (%)	DS_{COS} (%)
A 	2	2	F 	5	5	K 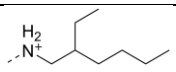	8 ± 0.13	6 ± 0.10
B 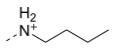	9 ± 1.38	9 ± 0.59	G 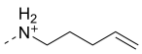	7 ± 1.20	4* ± 0.09	L 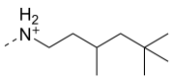	6 ± 0.48	5 ± 0.24
C 	11	10 ± 0.04	H 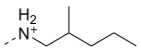	9 ± 1.33	7 ± 0.44	M 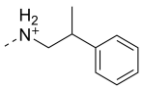	8 ± 0.60	7 ± 0.12
D 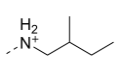	8 ± 1.13	8 ± 0.47	I 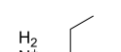	10 ± 0.86	9 ± 0.14	N 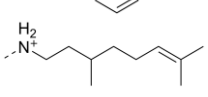	5	3*
E 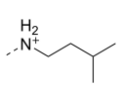	11 ± 0.95	11 ± 0.55	J 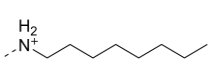	5 ± 0.94	4 ± 0.14	O 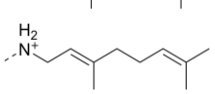	N.D.	N.D.*

An overview of all the synthesized and characterized derivatives is given in Table 1, together with their DS calculated via ^{1}H NMR (see Section S11.). Very similar values are obtained before and after

depolymerization, making the presence of insoluble NMR invisible fractions before depolymerization highly unlikely at these low degrees of substitution. This is in contrast with the NMR invisible fractions observed by Novoa-Carballal et al. for the chitosan-PEG copolymer (Novoa-Carballal et al., 2013). Moreover, a slight decrease in DS can be observed for certain samples after depolymerization. This might be attributed to the increased organic solubility of highly modified COS fractions, which no longer precipitate upon acetone addition (see section 2.3.3.2). As expected, due to the better-defined baseline/peaks, as well as the increased mobility of the less mobile atoms, the interpeak variability in DS decreased after depolymerization. A nice example of this phenomenon can be found in the supplementary information (e.g. see Section S11.2.). Finally, for nine of the fifteen chitosan derivatives a DS value within the range of 7-11 %, close to the envisioned 10 %, was obtained.

3. Conclusion

In this study, fifteen *N*-alkyl chitosan derivatives with varying linear, branched or unsaturated side chains, incorporating between three and ten carbon atoms, were successfully synthesized. A similar DS of approximately 10 % for nine compounds, determined via ^{1}H NMR, opens avenues for structure-activity studies on the effects of the different added alkyl chains. Next, these fifteen derivatives were subjected to selective acid-mediated depolymerization and subsequent fractionation by precipitation, obtaining high-purity *N*-alkyl COS hydrochloride salts. While small amounts of these modified COS were used for NMR structural elucidation, other unexplored properties, like foam stabilization or antimicrobial activity, will be investigated in the future. The reduced chain rigidity in these depolymerized compounds facilitated the unambiguous structural determination of thirteen compounds while indicating the structure of the remaining two, through a combination of various NMR techniques. NMR spectroscopy is a crucial tool for the analysis of modified polysaccharides, yet correct structural characterization of the obtained derivatives remains a big challenge. Notably, relying solely on ^{1}H NMR analysis, particularly on high molecular weight samples, may lead to inconclusive results, as demonstrated by the discrepancies in common assignments for this well-known class of chitosan derivatives found in the literature. Yet, these detailed structural characteristics are essential to realize the full potential of these biobased derivatives in the transition toward a climate-neutral future (Gericke et al., 2024).

4. Experimental

4.1. Materials

All chemicals and reagents were commercially available and obtained in analytical purity or higher from Tokyo Chemical Industry Co., Sigma-Aldrich and Carl Roth. Low molecular weight chitosan (KitoGreen®) (Mw = see Section S3., DA = 0.08, origin = fungal, 5.27 mmol NH_2/gram, insoluble fraction: 12-15 m% chitin-glucan complex) was supplied by KitoZyme (Herstal, Belgium) and utilized without further purification. The DA was determined based on ^{1}H NMR analyses (Lavertu et al., 2003). The amount of reactive NH_2 units in a gram of material was determined via an average of three potentiometric titrations (H. Wang et al., 2011). For a certain amount of equivalents, the obtained 5.27 mmol NH_2/gram was utilized to calculate the amount of reagent that should be added. All solvents were utilized as received without further purification. ^{11}B NMR was utilized to check for the presence of any leftover boron salts in the products obtained via reductive amination.

4.2. NMR analysis

1D and 2D NMR analyses were recorded at room temperature, unless stated otherwise, on a 400 MHz Bruker Avance III HD NanoBay, equipped with 1H/BB z-gradient probe (BBO, 5 mm), nuclear magnetic resonance (NMR) spectrometer. All spectra were processed using TOPSPIN 3.6.2. The standard pulse sequences supplied by Bruker were utilized for all 1D and 2D NMR analyses. The phasing of two-

dimensional ^{1}H-^{13}C HSQC NMR spectra was manually corrected if required. Samples were analyzed at 20 mg/mL in D_2O containing 1 vol% d-TFA.

4.3. Relative molecular weight determination

The relative molecular weight to pullulan standards of the starting chitosan together with the obtained products was determined via LC/GPC ELSD. For the calibration curve, 1 mg of a pullulan standard (342 Da, 1 kDa, 6 kDa, 10 kDa, 50 kDa, 110 kDa, 200 kDa, 400 kDa and 800 kDa, PSS standards kit) was dissolved in 1 mL of an 0.1 vol% TFA aqueous solution to obtain a final concentration of 1 mg/mL. For the chitosan samples, 5 mg of the sample was dissolved in 5 mL of an 0.1 vol% TFA aqueous solution to obtain a final concentration of 1 mg/mL. All solutions were left overnight to equilibrate and filtered using a 25 mm polyethersulfone (PES) syringe filter (0.22 µm membrane) before injection. 20 µL was automatically injected into an Agilent 1260 Infinity II HPLC system equipped with PSS NOVEMA Max analytical Linear M columns (10 µM particle size). A guard column and two GPC columns (8 x 300 mm) with a pore size of 100 Å, 3000 Å and 3000 Å were used respectively. The analyses were conducted at 25 °C with a flow rate of 0.5 mL/min. Detection was done using an Agilent 1260 Infinity ELSD detector, the evaporation temperature was set at 80 °C and the nebulizer temperature was at 42 °C with an evaporator gas flow of 2.5 standard liters per minute (SLM). All raw data were directly processed via Matlab R2023b (Sadao Mori, 1999).

4.4. Synthesis of *N*-alkyl chitosan

Two grams of chitosan was dissolved in 200 mL distilled water containing 1 vol% acetic acid and 0.05 w/v% cetylpyridinium chloride in a 500 mL round bottom flask by an overhead stirrer at 800 rpm. Afterward, 0.125 eq. of aldehyde (0.5 eq. for acetone) was added and the mixture was stirred for 1 hour. Next, 113 mg (0.1 eq.) of PICB was added and the mixture was stirred overnight. The following day, 20 mL of MeOH was added and the pH was adjusted to 3 with 1 N HCl. Subsequently, the mixture was stirred at 800 rpm for 2 hours at 60 °C to quench any residual PICB. Afterward, the chitosan derivative was precipitated by pouring the reaction mixture into 600 mL of acetone. Finally, the precipitate was collected via vacuum filtration, dried overnight at 50 °C and ground into a fine powder.

4.5. Oxidative depolymerization of (*N*-alkyl) chitosan

The oxidative depolymerization of (*N*-alkyl) chitosan was performed as previously described (Chapelle et al., 2019). Briefly, 62.5 mg of (*N*-alkyl) chitosan was dissolved overnight in 5 mL demineralized water containing 19.4 µL acetic acid. Next, 625 µL of a freshly prepared solution containing 0.2 eq. $NaNO_2$ was added and the mixture was stirred at 50 °C for three hours. Finally, as the obtained COS no longer precipitated upon the addition of acetone, COS were obtained after evaporation of the solvent.

4.6. Acid hydrolysis of (*N*-alkyl) chitosan

60 mg of (*N*-alkyl) chitosan was dissolved in 2 mL of 2 N HCl in a 20 mL capped vial. Afterward, the mixture was heated under reflux conditions for 24 hours. Next, the mixture was poured into 10 mL of acetone and the obtained precipitate was collected via centrifugation, dried overnight at 50 °C and ground into a fine powder.

CRediT authorship contribution statement

Casper Van Poucke: Conceptualization, Methodology, Formal analysis, Investigation, Data Curation, Writing - Original Draft, Writing – Review & Editing, Visualization, Project administration, Funding acquisition. **Evert Verdegem:** Investigation, Formal analysis. **Sven Mangelinckx:** Conceptualization, Methodology, Validation, Resources, Data Curation, Writing - Review & Editing, Supervision. **Christian V. Stevens:** Conceptualization, Methodology, Validation, Resources, Data Curation, Writing – Review & Editing, Supervision, Project administration, Funding acquisition.

Declaration of competing interest

The authors declare that they have no known competing financial interests or personal relationships that could have appeared to influence the work reported in this paper.

Acknowledgments

The authors acknowledge the Research Board of Ghent University (BOF21/DOC/019) for funding. We would like to thank Martha C. Mayorquín-Torres for the scientific discussions and Dieter Buyst for his help with the manual phasing of two-dimensional NMR data.

Data availability

Data will be made available on request.

References

Adams, J. P., Alder, C. M., Andrews, I., Bullion, A. M., Campbell-Crawford, M., Darcy, M. G., Hayler, J. D., Henderson, R. K., Oare, C. A., Pendrak, I., Redman, A. M., Shuster, L. E., Sneddon, H. F., & Walker, M. D. (2013). Development of GSK's reagent guides – embedding sustainability into reagent selection. *Green Chem.*, *15*(6), 1542–1549. https://doi.org/10.1039/C3GC40225H

Allan, G. G., & Peyron, M. (1995). Molecular weight manipulation of chitosan I: kinetics of depolymerization by nitrous acid. *Carbohydrate Research*, *277*(2), 257–272. https://doi.org/10.1016/0008-6215(95)00207-A

Ando, N., Yamamoto, Y., Oda, J., & Inouye, Y. (1979). Effect of Complexation by Crown Ethers on Anisochrony of Diastereotopic Groups in NMR Spectra. *Bulletin of the Chemical Society of Japan*, *52*(8), 2369–2371. https://doi.org/10.1246/bcsj.52.2369

Anthonsen, M. W., & Smidsrød, O. (1995). Hydrogen ion titration of chitosans with varying degrees of N-acetylation by monitoring induced 1H-NMR chemical shifts. *Carbohydrate Polymers*, *26*(4), 303–305. https://doi.org/10.1016/0144-8617(95)00010-5

Benediktsdóttir, B. E., Gudjónsson, T., Baldursson, Ó., & Másson, M. (2014). N-alkylation of highly quaternized chitosan derivatives affects the paracellular permeation enhancement in bronchial epithelia in vitro. *European Journal of Pharmaceutics and Biopharmaceutics*, *86*(1), 55–63. https://doi.org/10.1016/j.ejpb.2013.04.002

Bobu, E., Raluca, N., Lupei, M., Ciolacu, F. L., & Desbrieres, J. (2011). Synthesis and characterization of n-alkyl chitosan for papermaking applications. *Cellulose Chemistry and Technology*, *45*(9–10), 619–625.

Borch, R. F., Bernstein, M. D., & Durst, H. D. (1971). Cyanohydridoborate anion as a selective reducing agent. *Journal of the American Chemical Society*, *93*(12), 2897–2904. https://doi.org/10.1021/ja00741a013

Chapelle, C., David, G., Caillol, S., Negrell, C., Durand, G., Desroches le Foll, M., & Trombotto, S. (2019). Water-Soluble 2,5-Anhydro-d-mannofuranose Chain End Chitosan Oligomers of a Very Low Molecular Weight: Synthesis and Characterization. *Biomacromolecules*, *20*(12), 4353–4360. https://doi.org/10.1021/acs.biomac.9b01003

Cook, M., Viola, M., Vecchies, F., Sacco, P., Furlani, F., Marsich, E., & Donati, I. (2020). N-isopropyl chitosan. A pH- and thermo-responsive polysaccharide for gel formation. *Carbohydrate Polymers*, *230*, 115641. https://doi.org/10.1016/j.carbpol.2019.115641

Cosenza, V. A., Navarro, D. A., & Stortz, C. A. (2011). Usage of α-picoline borane for the reductive amination of carbohydrates. *ARKIVOC*, *2011*(7), 182–194. https://doi.org/10.3998/ark.5550190.0012.716

Coudurier, M., Faivre, J., Crépet, A., Ladavière, C., Delair, T., Schatz, C., & Trombotto, S. (2020). Reducing-End Functionalization of 2,5-Anhydro-d-mannofuranose-Linked Chitooligosaccharides by Dioxyamine: Synthesis and Characterization. *Molecules (Basel, Switzerland)*, *25*(5), 1143. https://doi.org/10.3390/molecules25051143

de Britto, D., & de Assis, O. B. G. (2007). Synthesis and mechanical properties of quaternary salts of chitosan-based films for food application. *International Journal of Biological Macromolecules*, *41*(2), 198–203. https://doi.org/10.1016/j.ijbiomac.2007.02.005

Demir-Yilmaz, I., Ftouhi, M. S., Balayssac, S., Guiraud, P., Coudret, C., & Formosa-Dague, C. (2023). Bubble functionalization in flotation process improve microalgae harvesting. *Chemical Engineering Journal*, *452*, 139349. https://doi.org/10.1016/j.cej.2022.139349

Desbrières, J., Martinez, C., & Rinaudo, M. (1996). Hydrophobic derivatives of chitosan: Characterization and rheological behaviour. *International Journal of Biological Macromolecules*, *19*(1), 21–28. https://doi.org/10.1016/0141-8130(96)01095-1

Domard, A., & Cartier, N. (1989). Glucosamine oligomers: 1. Preparation and characterization. *International Journal of Biological Macromolecules*, *11*(5), 297–302. https://doi.org/10.1016/0141-8130(89)90023-8

Dowling, M. B., Kumar, R., Keibler, M. A., Hess, J. R., Bochicchio, G. V, & Raghavan, S. R. (2011). A self-assembling hydrophobically modified chitosan capable of reversible hemostatic action. *Biomaterials*, *32*(13), 3351–3357. https://doi.org/10.1016/j.biomaterials.2010.12.033

Einbu, A., & Vårum, K. M. (2007). Depolymerization and De-N-acetylation of Chitin Oligomers in Hydrochloric Acid. *Biomacromolecules*, *8*(1), 309–314. https://doi.org/10.1021/bm0608535

Einbu, A., & Vårum, K. M. (2008). Characterization of Chitin and Its Hydrolysis to GlcNAc and GlcN. *Biomacromolecules*, *9*(7), 1870–1875. https://doi.org/10.1021/bm8001123

Garinha, I., Duarte, P., Pimentel, A., Plotnikova, E., Chagas, B., Mafra, L., Grandfils, C., Freitas, F., Fortunato, E., & Reis, M. A. M. (2015). Chitin–glucan complex production by Komagataella pastoris: Downstream optimization and product characterization. *Carbohydrate Polymers*, *130*, 455–464. https://doi.org/10.1016/j.carbpol.2015.05.034

Fukamizo, T., Ohtakara, A., Mitsutomi, M., & Goto, S. (1991). NMR spectra of partially deacetylated chitotrisaccharides. *Agricultural and Biological Chemistry*, *55*(10), 2653–2655.

Gericke, M., Amaral, A. J. R., Budtova, T., De Wever, P., Groth, T., Heinze, T., Höfte, H., Huber, A., Ikkala, O., Kapuśniak, J., Kargl, R., Mano, J. F., Másson, M., Matricardi, P., Medronho, B., Norgren, M., Nypelö, T., Nyström, L., Roig, A., … Fardim, P. (2024). The European Polysaccharide Network of Excellence (EPNOE) research roadmap 2040: Advanced strategies for exploiting the vast potential of polysaccharides as renewable bioresources. *Carbohydrate Polymers*, *326*, 121633. https://doi.org/10.1016/j.carbpol.2023.121633

Hanashima, S., Ikeda, A., Tanaka, H., Adachi, Y., Ohno, N., Takahashi, T., & Yamaguchi, Y. (2014). NMR study of short β(1-3)-glucans provides insights into the structure and interaction with Dectin-1. *Glycoconjugate Journal*, *31*(3), 199–207. https://doi.org/10.1007/s10719-013-9510-x

Ishino, R., & Kumanotani, J. (1974). Synthesis of hydroxycitronellal. Hydration and subsequent hydrolysis of imines, enamines, or oxazolidines prepared from citronellal and amines. *The Journal of Organic Chemistry*, *39*(1), 108–111. https://doi.org/10.1021/jo00915a028

[6] Jia, Z., shen, D., & Xu, W. (2001). Synthesis and antibacterial activities of quaternary ammonium salt of chitosan. *Carbohydrate Research*, *333*(1), 1–6. https://doi.org/10.1016/S0008-6215(01)00112-4

[7] Kalliola, S., Repo, E., Srivastava, V., Zhao, F., Heiskanen, J. P., Sirviö, J. A., Liimatainen, H., & Sillanpää, M. (2018). Carboxymethyl Chitosan and Its Hydrophobically Modified Derivative as pH-Switchable Emulsifiers. *Langmuir*, *34*(8), 2800–2806. https://doi.org/10.1021/acs.langmuir.7b03959

[8] Kim, C. H., Choi, J. W., Chun, H. J., & Choi, K. S. (1997). Synthesis of chitosan derivatives with quaternary ammonium salt and their antibacterial activity. *Polymer Bulletin*, *38*(4), 387–393. https://doi.org/10.1007/s002890050064

[9] Kong, M., Chen, X. G., Xing, K., & Park, H. J. (2010). Antimicrobial properties of chitosan and mode of action: A state of the art review. *International Journal of Food Microbiology*, *144*(1), 51–63. https://doi.org/10.1016/j.ijfoodmicro.2010.09.012

[10] Kurita, Y., & Isogai, A. (2010). Reductive N-alkylation of chitosan with acetone and levulinic acid in aqueous media. *International Journal of Biological Macromolecules*, *47*(2), 184–189. https://doi.org/10.1016/j.ijbiomac.2010.05.001

[11] Lavertu, M., Xia, Z., Serreqi, A. N., Berrada, M., Rodrigues, A., Wang, D., Buschmann, M. D., & Gupta, A. (2003). A validated 1H NMR method for the determination of the degree of deacetylation of chitosan. *Journal of Pharmaceutical and Biomedical Analysis*, *32*(6), 1149–1158. https://doi.org/https://doi.org/10.1016/S0731-7085(03)00155-9

[12] LeHoux, J.-G., & Dupuis, G. (2007). Recovery of chitosan from aqueous acidic solutions by salting-out: Part 1. Use of inorganic salts. *Carbohydrate Polymers*, *68*(2), 295–304. https://doi.org/https://doi.org/10.1016/j.carbpol.2006.12.008

[13] Lepeltier, E., Loretz, B., Desmaële, D., Zapp, J., Herrmann, J., Couvreur, P., & Lehr, C.-M. (2015). Squalenoylation of Chitosan: A Platform for Drug Delivery? *Biomacromolecules*, *16*(9), 2930–2939. https://doi.org/10.1021/acs.biomac.5b00840

[14] Ma, G., Yang, D., Zhou, Y., Xiao, M., Kennedy, J. F., & Nie, J. (2008). Preparation and characterization of water-soluble N-alkylated chitosan. *Carbohydrate Polymers*, *74*(1), 121–126. https://doi.org/10.1016/j.carbpol.2008.01.028

[15] Ma, & Warnhoff, E. W. (1965). ON THE USE OF NUCLEAR MAGNETIC RESONANCE FOR THE DETECTION, ESTIMATION, AND CHARACTERIZATION OF N-METHYL GROUPS. *CJC Western University Virtual Compilation*, *1*(1), 1849–1869. https://doi.org/10.1139/v65-242

[16] Mati-Baouche, N., Delattre, C., de Baynast, H., Grédiac, M., Mathias, J.-D., Ursu, A. V., Desbrières, J., & Michaud, P. (2019). Alkyl-Chitosan-Based Adhesive: Water Resistance Improvement. *Molecules (Basel, Switzerland)*, *24*(10), 1987. https://doi.org/10.3390/molecules24101987

[17] Mo, I. V., Dalheim, M. Ø., Aachmann, F. L., Schatz, C., & Christensen, B. E. (2020). 2,5-Anhydro-d-Mannose End-Functionalized Chitin Oligomers Activated by Dioxyamines or Dihydrazides as Precursors of Diblock Oligosaccharides. *Biomacromolecules*, *21*(7), 2884–2895. https://doi.org/10.1021/acs.biomac.0c00620

[18] Novoa-Carballal, R., Riguera, R., & Fernandez-Megia, E. (2013). Disclosing an NMR-Invisible Fraction in Chitosan and PEGylated Copolymers and Its Role on the Determination of Degrees of Substitution. *Molecular Pharmaceutics*, *10*(8), 3225–3231. https://doi.org/10.1021/mp400267m

546 de Paula, H. C. B., Silva, R. B. C., Santos, C. M., Dantas, F. D. S., de Paula, R. C. M., de Lima, L. R. M., de Oliveira,
547 E. F., Figueiredo, E. A. T., & Dias, F. G. B. (2020). Eco-friendly synthesis of an alkyl chitosan derivative.
548 *International Journal of Biological Macromolecules*, *163*, 1591–1598.
549 https://doi.org/10.1016/j.ijbiomac.2020.08.058

550 Prat, D., Wells, A., Hayler, J., Sneddon, H., McElroy, C. R., Abou-Shehada, S., & Dunn, P. J. (2016). CHEM21
551 selection guide of classical- and less classical-solvents. *Green Chem.*, *18*(1), 288–296.
552 https://doi.org/10.1039/C5GC01008J

553 Rabea, E. I., Badawy, M. E. I., Rogge, T. M., Stevens, C. V, Höfte, M., Steurbaut, W., & Smagghe, G. (2005).
554 Insecticidal and fungicidal activity of new synthesized chitosan derivatives. *Pest Management Science*,
555 *61*(10), 951–960. https://doi.org/10.1002/ps.1085

556 Ramachandran, P. V., Hamann, H. J., Lin, R., & Singh, A. (2023). Scalable, Green Synthesis of Heteroaromatic
557 Amine-boranes. *Organic Process Research & Development*, *27*(4), 775–783.
558 https://doi.org/10.1021/acs.oprd.3c00031

559 Sadao Mori, H. G. B. (1999). *Size Exclusion Chromatography*. Springer-Verlag Berlin Heidelberg 1999.
560 https://doi.org/https://doi.org/10.1007/978-3-662-03910-6

561 Sahariah, P., Benediktssdóttir, B. E., Hjálmarsdóttir, M. Á., Sigurjonsson, O. E., Sørensen, K. K., Thygesen, M.
562 B., Jensen, K. J., & Másson, M. (2015). Impact of Chain Length on Antibacterial Activity and
563 Hemocompatibility of Quaternary N-Alkyl and N,N-Dialkyl Chitosan Derivatives. *Biomacromolecules*,
564 *16*(5), 1449–1460. https://doi.org/10.1021/acs.biomac.5b00163

565 Sahariah, P., & Másson, M. (2017). Antimicrobial Chitosan and Chitosan Derivatives: A Review of the
566 Structure–Activity Relationship. *Biomacromolecules*, *18*(11), 3846–3868.
567 https://doi.org/10.1021/acs.biomac.7b01058

568 Sajomsang, W., Gonil, P., & Tantayanon, S. (2009). Antibacterial activity of quaternary ammonium chitosan
569 containing mono or disaccharide moieties: Preparation and characterization. *International Journal of*
570 *Biological Macromolecules*, *44*(5), 419–427. https://doi.org/10.1016/j.ijbiomac.2009.03.003

571 Sajomsang, W., Tantayanon, S., Tangpasuthadol, V., Thatte, M., & Daly, W. H. (2008). Synthesis and
572 characterization of N-aryl chitosan derivatives. *International Journal of Biological Macromolecules*,
573 *43*(2), 79–87. https://doi.org/10.1016/j.ijbiomac.2008.03.010

574 Sarneski, J. E., Surprenant, H. L., Molen, F. K., & Reilley, C. N. (1975). Chemical shifts and protonation shifts
575 in carbon-13 nuclear magnetic resonance studies of aqueous amines. *Analytical Chemistry*, *47*(13),
576 2116–2124. https://doi.org/10.1021/ac60363a010

577 Yashiwa, H., & Shigemasa, Y. (1999). Chemical modification of chitin and chitosan 2: preparation and water
578 soluble property of N-acylated or N-alkylated partially deacetylated chitins. *Carbohydrate Polymers*,
579 *39*(2), 127–138. https://doi.org/10.1016/S0144-8617(98)00167-2

580 Sato, S., Sakamoto, T., Miyazawa, E., & Kikugawa, Y. (2004). One-pot reductive amination of aldehydes and
581 ketones with α-picoline-borane in methanol, in water, and in neat conditions. *Tetrahedron*, *60*(36),
582 7899–7906. https://doi.org/https://doi.org/10.1016/j.tet.2004.06.045

583 Sugiyama, H., Hisamichi, K., Sakai, K., Usui, T., Ishiyama, J.-I., Kudo, H., Ito, H., & Senda, Y. (2001). The
584 conformational study of chitin and chitosan oligomers in solution. *Bioorganic & Medicinal Chemistry*,
585 *9*(2), 211–216. https://doi.org/10.1016/S0968-0896(00)00236-4

[586] Chongngam, M., & McClements, D. J. (2005). Influence of pH, Ionic Strength, and Temperature on Self-
587 Association and Interactions of Sodium Dodecyl Sulfate in the Absence and Presence of Chitosan.
588 *Langmuir*, *21*(1), 79–86. https://doi.org/10.1021/la048711o

[589] Sømmeraas, K., Vårum, K. M., Christensen, B. E., & Smidsrød, O. (2001). Preparation and characterisation of
590 oligosaccharides produced by nitrous acid depolymerisation of chitosans. *Carbohydrate Research*,
591 *333*(2), 137–144. https://doi.org/10.1016/S0008-6215(01)00130-6

[592] Triunfo, M., Tafi, E., Guarnieri, A., Salvia, R., Scieuzo, C., Hahn, T., Zibek, S., Gagliardini, A., Panariello, L.,
593 Coltelli, M. B., De Bonis, A., & Falabella, P. (2022). Characterization of chitin and chitosan derived from
594 Hermetia illucens, a further step in a circular economy process. *Scientific Reports*, *12*(1), 6613.
595 https://doi.org/10.1038/s41598-022-10423-5

[596] Van Poucke, C., Vandeputte, A., Mangelinckx, S., & Stevens, C. V. (2023). Green mechanochemical synthesis
597 of water-soluble N-sulfonated chitosan. *Green Chem.*, *25*, 4271–4281.
598 https://doi.org/10.1039/D3GC00549F

[599] Varma, A. J., Deshpande, S. V, & Kennedy, J. F. (2004). Metal complexation by chitosan and its derivatives: a
600 review. *Carbohydrate Polymers*, *55*(1), 77–93.
601 https://doi.org/https://doi.org/10.1016/j.carbpol.2003.08.005

[602] Vårum, K. M., Ottøy, M. H., & Smidsrød, O. (2001). Acid hydrolysis of chitosans. *Carbohydrate Polymers*,
603 *46*(1), 89–98. https://doi.org/10.1016/S0144-8617(00)00288-5

[604] Venkataraman, P., Tang, J., Frenkel, E., McPherson, G. L., He, J., Raghavan, S. R., Kolesnichenko, V., Bose, A.,
605 & John, V. T. (2013). Attachment of a Hydrophobically Modified Biopolymer at the Oil–Water Interface
606 in the Treatment of Oil Spills. *ACS Applied Materials & Interfaces*, *5*(9), 3572–3580.
607 https://doi.org/10.1021/am303000v

[608] Wang, H., Qian, C., & Roman, M. (2011). Effects of pH and Salt Concentration on the Formation and
609 Properties of Chitosan–Cellulose Nanocrystal Polyelectrolyte–Macroion Complexes.
610 *Biomacromolecules*, *12*(10), 3708–3714. https://doi.org/10.1021/bm2009685

[611] Wang, P., Lv, X., Zhang, B., Wang, T., Wang, C., Sun, J., Zhang, K., Wu, Y., Zhao, J., & Zhang, Y. (2021).
612 Simultaneous determination of molar degree of substitution and its distribution fraction, degree of
613 acetylation in hydroxypropyl chitosan by 1H NMR spectroscopy. *Carbohydrate Polymers*, *263*, 117950.
614 https://doi.org/10.1016/j.carbpol.2021.117950

[615] Yalpani, M., & Hall, L. D. (1984). Some chemical and analytical aspects of polysaccharide modifications. III.
616 Formation of branched-chain, soluble chitosan derivatives. *Macromolecules*, *17*(3), 272–281.
617 https://doi.org/10.1021/ma00133a003